THE JOURNAL OF PHYSICAL CHEMISTRY C

Article

Cite This: J. Phys. Chem. C XXXX, XXX, XXX−XXX

pubs.acs.org/JPCC

Bidirectional Electronic Tuning of Single-Layer MoS_2 with Conjugated Organochalcogens

Peijian Wang,[†,‡,⊥] Ryan Selhorst,[§,⊥] Todd Emrick,[§] Ashwin Ramasubramaniam,[∥] and Michael D. Barnes*[,†,‡]

[†]Department of Chemistry and [‡]Department of Physics, University of Massachusetts, Amherst, 710 North Pleasant Street, Amherst, Massachusetts 01003, United States

[§]Polymer Science and Engineering Department, 120 Governors Drive, Amherst, Massachusetts 01003, United States

[∥]Department of Mechanical and Industrial Engineering, University of Massachusetts, Amherst, 160 Governors Drive, Amherst, Massachusetts 01003, United States

Supporting Information

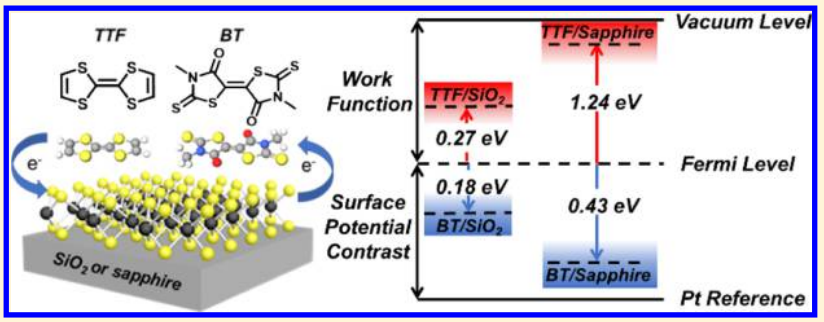

ABSTRACT: We report a bidirectional tuning of the electronic properties of single-layer molybdenum disulfide (MoS_2) by n-doping with the electron donating tetrathiafulvalene (TTF) and p-doping with the electron accepting bithiazolidinylidene (BT). Using Kelvin probe force microscopy (KPFM), we spatially monitored changes in the work function of monolayer MoS_2 on silicon oxide (SiO_2) and sapphire (Al_2O_3). KPFM, in conjunction with spectroscopic characterization, showed MoS_2 work function shifts as significant as 1.24 eV for TTF doping, and 0.43 eV for BT doping, when Al_2O_3 was employed as the underlying substrate. Less dramatic changes were observed for MoS_2 on SiO_2/Si, revealing a significant impact of substrate selection on the electronic properties of this 2D material. High-level computations helped guide experiments on chemical modulation of the electronic properties of this transition-metal dichalcogenide.

INTRODUCTION

Transition-metal dichalcogenides (TMDCs), such as MoS_2 and WSe_2, are layered 2D semiconductors possessing both electron (n-type) and hole (p-type) conduction characteristics.[1−3] TMDCs exhibit an inherent, layer-dependent band gap, transitioning from an indirect band gap of 1.2 eV to a direct band gap of 1.8 eV at monolayer thickness.[4] These properties promote integration of TMDCs into electronic devices; for example, in field effect transistors (FETs), single-layer MoS_2 displays high electron mobility (~200 $cm^2\ V^{-1}\ s^{-1}$)[5] and large current on/off ratios (~10^8).[4,5] Beyond FETs, further integration of TMDCs into (opto)electronic devices will hinge on manipulating their carrier density and work function (WF). Controlling WF, the energy associated with promoting an electron from the Fermi level (electron chemical potential) to the vacuum level, is essential for enabling precise device engineering. For example, the difference in WF between the active layer and the electrode in photovoltaic devices significantly influences the open circuit voltage and charge injection/extraction processes.[6−9] To date, modification of TMDC WF using mechanical strain, heterostructure fabrication, or transition metal substrates has been demonstrated.[10−15] However, these methods are cumbersome, typically involving deposition or use of transition metal substrates, which are not scalable for 2D materials devices. Chemical doping is an alternative method for modifying TMDCs, providing a solution processible platform that alleviates multistep processing. For example, MoS_2 that was p-doped with perfluorinated thiols exhibited ambipolar transistor characteristics; when reacted with gold salts, carrier inversion from n-type to p-type was reported.[16−18] While these methods irreversibly alter both the physical and electronic structure of the material, doping with small molecules and polymers by noncovalent physisorption would, in principle, circumvent these problems and introduce the potential for spatially patterned electronic properties needed in next-generation TMDC-based devices.[19]

Received: November 7, 2018
Revised: December 11, 2018
Published: December 20, 2018

DOI: 10.1021/acs.jpcc.8b10826
J. Phys. Chem. C XXXX, XXX, XXX−XXX

We previously reported a WF decrease (resulting from n-doping) of multilayer MoS_2 when in contact with electron-donating polymers-containing tetrathiafulvalene (TTF) moieties.[20] While experiments confirmed n-doping of MoS_2 with TTF, the magnitude of the WF shift differed significantly from theoretical calculations. We hypothesize that this disparity is a result of doping multilayer versus monolayer MoS_2—a parameter that was not controlled closely in previous experiments. We also note that our previous theoretical insights include adsorption at defect sites (sulfur vacancies) in MoS_2. These high energy vacancies provide different local electronic properties that are hypothesized to influence the doping efficiency at these sites. While defects influence local WF modification, we focus our investigation on the electronic impact of physisorbed dopants. In this paper, we employed epitaxially grown monolayer MoS_2 to examine n- and p-type dopants on the directional shift of the Fermi level. Using TTF and bithiazolidinylidene (BT) as n- and p-dopants, respectively, we observed bidirectional tuning of the Fermi level, manifested as a shift in the surface potential contrast (SPC) recorded by Kelvin probe force microscopy (KPFM). The underlying substrate (SiO_2 vs Al_2O_3) played a significant role on the magnitude of WF shift. On the basis of this, a physical picture is proposed to explain the substrate dependence and experimental versus theoretical results associated with the magnitude of electronic modulation arising from doping MoS_2.

RESULTS AND DISCUSSION

The layer thickness of MoS_2, grown by chemical vapor deposition (CVD) on SiO_2/Si and sapphire (Al_2O_3), was assessed by Raman spectroscopy. The Raman spectrum of MoS_2 contains two characteristic transitions in the low frequency region: an in-plane (E_{2g}) and out-of-plane (A_{1g}) stretch. Decreasing the number of MoS_2 layers causes the E_{2g} peak to shift to higher energy and the A_{1g} peak to lower energy, thus reducing the energy difference between the two peaks. Figure 1a shows Raman spectra of single-layer MoS_2 on SiO_2/Si and sapphire; the E_{2g} peak is centered at 385 cm^{-1} and the A_{1g} peak at 405 cm^{-1}, a peak separation of ~20 cm^{-1} that agrees with literature reports of monolayer MoS_2.[11,21] Figure 1b shows the photoluminescence (PL) spectra of MoS_2 on SiO_2/Si and sapphire with maximum PL intensity at 660 nm found in monolayer MoS_2, also consistent with previous reports.[22,23] To investigate the directional Fermi-level tuning on MoS_2, the organic dopants TTF (n-dopant) and BT (p-dopant) were selected for their electron donating and accepting properties, respectively. The sulfur-rich structures of these donor and acceptor molecules were anticipated to promote noncovalent interactions with the basal plane of MoS_2.[20] The BT derivatives were synthesized as described in the Methods section.[24] KPFM, employed to evaluate doping of MoS_2 with TTF- and BT-dopants, is a scanning probe technique that exploits a capacitive interaction between a metal-coated cantilever probe and the sample. This interaction has a first harmonic component correlating to the WF difference between the metal coating (Pt) and the material being probed (details in Supporting Information).[25] Quantitative measurement of WF of the sample is then determined by calibration of the probe WF, with the WF difference measured as a change in SPC.[26−28] Furthermore, KPFM allows measurement beyond just the contacting interfaces, possessing a penetration depth of approximately 100 nm, ensuring WF measurement of MoS_2 and not simply the small molecule coating.[29−31]

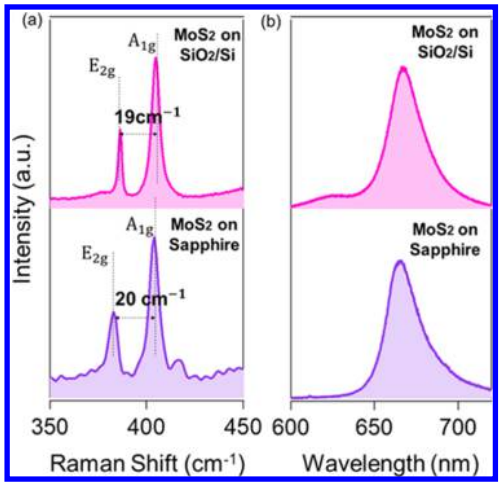

Figure 1. (a) Raman spectra of MoS_2 on SiO_2/Si (top) and sapphire (bottom) showing the in-plane and out-of-plane stretches. (b) PL spectra of MoS_2 on SiO_2/Si (top) and sapphire (bottom) showing peak intensity at 660 nm, indicative of monolayer MoS_2.

The single-layer MoS_2 substrates were scanned both before and after drop-casting the TTF and BT dopants from dilute methanol solutions (0.005 mg/mL). Figure 2 shows the surface height and SPC images before and after drop-casting TTF on the MoS_2-covered substrate. Each experiment was repeated using either sapphire or SiO_2/Si as the underlying substrate. Figure 2a,b shows the height images of an MoS_2 flake on SiO_2/Si and Figure 2c,d shows the surface potential images of the same area of MoS_2 before and after addition of TTF. The step height of the flake from the images was approximately 0.8−1.0 nm (Figure S1) and a WF of 5.1−5.2 eV was measured before addition of the dopants, consistent with WF values for single-layer MoS_2 reported in the literature.[11,20,32] Upon addition of TTF to MoS_2, a 9−10 nm height change was observed (height histograms in Figures S3 and S5) and KPFM recorded a 0.27 eV upshift in SPC, corresponding to n-doping of MoS_2. Interestingly, when sapphire was used as the underlying substrate (Figure 2e−h), the magnitude of the SPC shift increased significantly to 1.24 eV, approaching values predicted by theory (1.64 eV).[20] Control experiments (Figure S2) showed that methanol, used to cast TTF and BT dopants from solution, had very little effect on the WF of MoS_2 and that the observed doping is nearly exclusively because of the contact of MoS_2 with the organic dopants. MoS_2 substrates coated with BT showed the opposite WF shifts, indicative of p-doping. The height profiles (Figure 3a,b,e,f) show a clear change between the MoS_2 flake and the substrate before and after addition of methyl BT (m-BT) to the substrate. After applying a thin coating of m-BT to the surface (Figures S7 and S9), MoS_2 on SiO_2/Si showed a 0.18 eV reduction in SPC (Figure 3c,d) while MoS_2 on sapphire displayed a much greater reduction (0.43 eV) in SPC (Figure 3g,h). Interestingly, coating MoS_2 with a BT derivative containing *n*-butyl side chains produced lower WF shifts than the methyl derivative (Figures S11 and S12). We speculate that the smaller WF changes from butyl BT (b-BT) stem from the higher amount of insulting alkyl functionality per molecule, diminishing the electron withdrawing nature of BT. On both substrates, the reversibility of doping is demonstrated by

DOI: 10.1021/acs.jpcc.8b10826
J. Phys. Chem. C XXXX, XXX, XXX−XXX

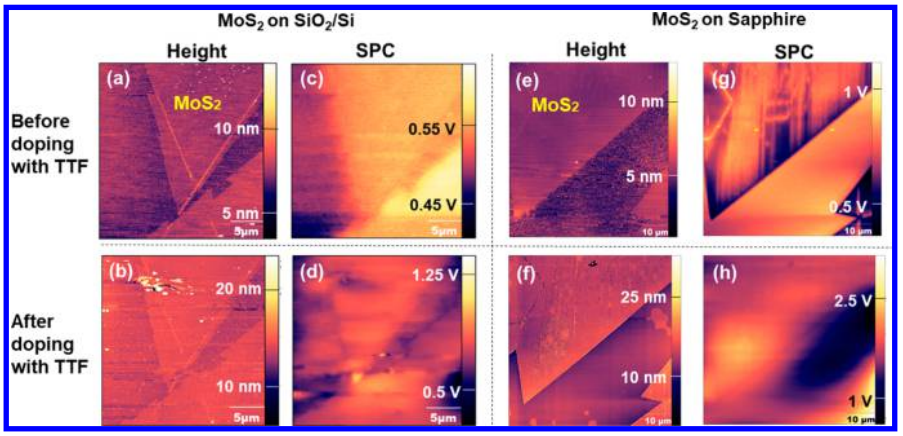

Figure 2. Surface height and KPFM images of monolayer MoS_2 on Si/SiO_2: (a) surface height before doping with TTF; (b) surface height after doping with TTF; (c) surface potential before doping with TTF; (d) surface potential after doping with TTF. Sapphire: (e) surface height before doping with TTF; (f) surface height after doping with TTF; (g) surface potential before doping with TTF; (h) surface potential after doping with TTF.

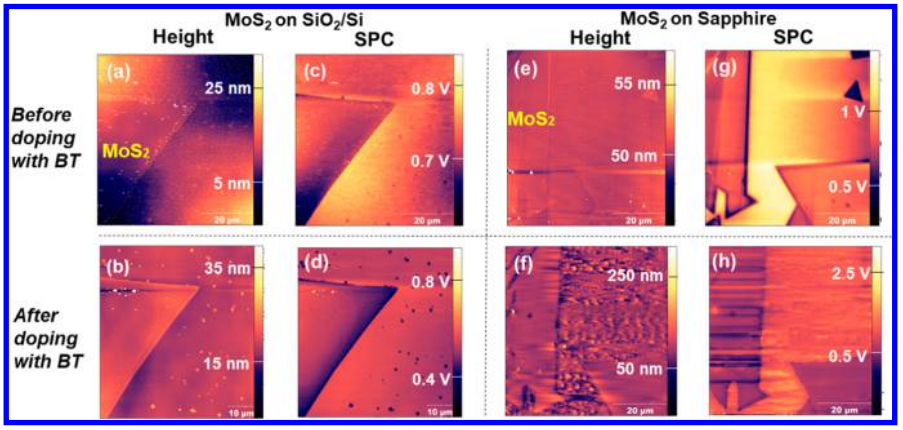

Figure 3. Surface height and KPFM images of monolayer MoS_2 on Si/SiO_2: (a) surface height before doping with m-BT; (b) surface height after doping with m-BT; (c) surface potential before doping with m-BT; (d) surface potential after doping with m-BT. Sapphire: (e) surface height before doping with m-BT; (f) surface height after doping with m-BT; (g) surface potential before doping with m-BT; (h) surface potential after doping with m-BT.

recovery of the original WF after rinsing and sonicating the MoS_2 substrates in chloroform (Figures S4, S6, S8, S10, S13, and S15). The doping experiments revealed a large dependence of WF shift on the composition of the underlying substrate. Figure 4a summarizes the SPC shifts of MoS_2 doped by TTF and BT derivatives by extracting the SPC values from the images of the scanned areas and displaying the SPC shifts as histograms. These large WF shifts are striking and show that the electronic properties of MoS_2 may be tailored directionally, over a wide range, by noncovalent adsorption of different dopants and the use of different substrates.

To further confirm TTF and BT doping of MoS_2, PL spectroscopy was performed on monolayer MoS_2 before and after coating with these organic dopants. Upon coating with TTF, the intensity of the A-peak (666 nm) decreased and shifted to longer wavelengths (4 nm), indicating n-doping,[23,32] while the B-peak (623 nm) intensity increased with no shift in wavelength (Figure 4b, top). For BT doping, the A-and B-peak intensities both decreased and the A peak shifted to shorter wavelengths (5 nm), while the B-peaks did not shift, indicating p-doping (Figure 4b bottom).[23,32] The PL shifts in the A-peak from doping are caused from the increase or decrease of the trion (bound exciton and electron) component after the addition or depletion of charge.[23,33] The wavelength shift for BT doping is consistent with literature reports on p-doping of MoS_2; however, the decrease in PL intensity is not.[23] This PL decrease may result from overlapping BT absorption with MoS_2 photoexcitation (absorption and PL spectra of TTF and BT in Figures S16–S19). It is interesting to point out that simulations of carrier doping in pristine (defect-free) MoS_2, using high-level density functional theory, predict an n-type doping for both TTF and BT molecules, contrary to the experimental observations reported here. However, recent unpublished X-ray photoelectron spectroscopy measurements by Naveh[34] on WSe_2 have shown that pendent groups that are anticipated to be n-dopants may impart a Fermi-level lowering, consistent with p-type doping. This counterintuitive effect appears to be correlated with chalcogen vacancy defects in the TMDC, although the mechanism of this effect is yet clear, work is underway to probe this in more detail. Nevertheless, our results indicate yet another route to Fermi-level tuning via complementary defect engineering and surface functionalization of MoS_2.

Figure 5 presents our physical picture of the observed coating-induced WF shifts of MoS_2. Electron transfer between the TTF or BT dopants and MoS_2 generates a dipole that is directed outward from MoS_2 for TTF (Figure 5a) and inward toward MoS_2 for BT (Figure 5b); the former dipole

DOI: 10.1021/acs.jpcc.8b10826
J. Phys. Chem. C XXXX, XXX, XXX−XXX

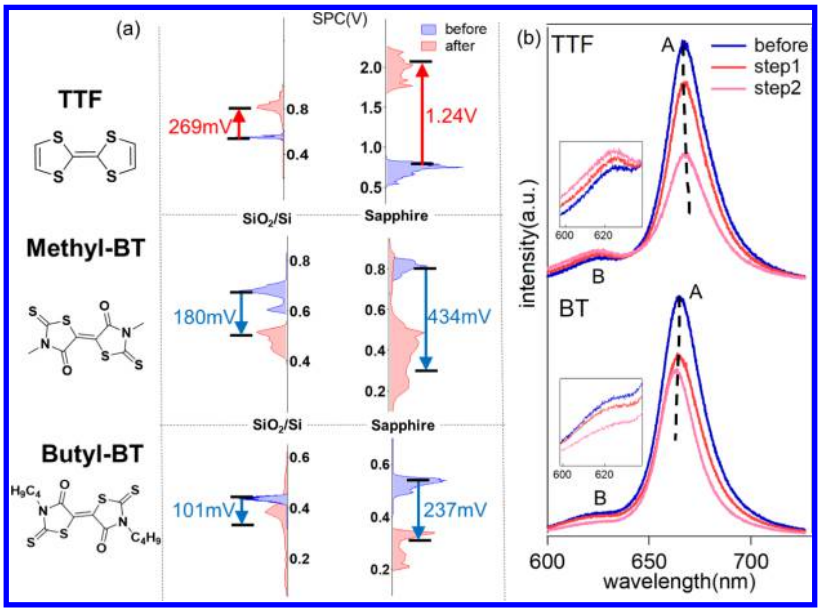

Figure 4. (a) Changes in SPC of single layer MoS_2 before and after doping with TTF, methyl-BT, and *n*-butyl-BT. The left portion shows the results of doping with TTF and BTs on SiO_2/Si and the right portion shows the results from doping MoS_2 with TTF and BTs on sapphire; (b) PL spectra of single layer MoS_2 on SiO_2/Si before coating and after one and two additions of TTF and BT solutions, showing wavelength shifts corresponding to n- or p-doping. Insets show the MoS_2 B peak.

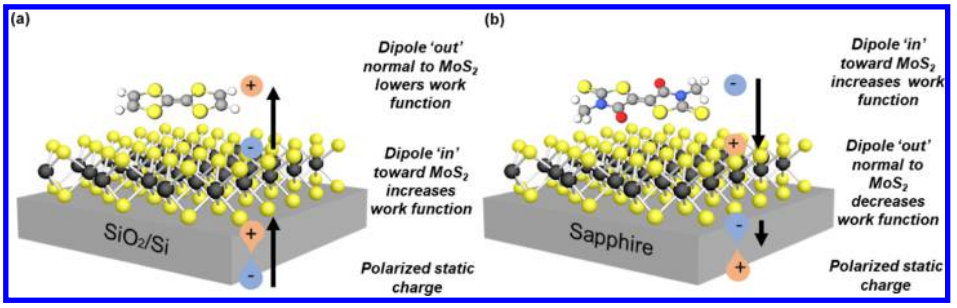

Figure 5. Schematic of dipole and induced static polarization responsible for WF shifts in MoS_2 after doping. (a) TTF donates electrons by charge transfer to MoS_2; (b) electron transfer gives rise to a dipole between the dopant and MoS_2, which induces a dipole at the dielectric/semiconductor interface from static charge. This polarized static charge effectively screens the measured WF of MoS_2, and the screening strength depends on dielectric constant of the underlying substrate.

orientation decreases the MoS_2 WF, whereas the latter increases the WF.[35] The WF change due to interfacial dipoles is given by $\Delta WF = \frac{\sigma_d}{\varepsilon_0 \varepsilon}$, where σ_d is the dipole moment area density, ε_0 is the permittivity of vacuum, and ε is the relative permittivity of the dielectric. The dipoles generated by contact of the 2D material and organic dopant induce a polarized static charge, forming opposing dipoles at the substrate/semiconductor interface, effectively screening the measured surface potential. Increasing the dielectric constant reduces the magnitude of this screening effect, leading to a smaller WF offset and amplifying the WF shift in the 2D material. Because sapphire has a dielectric constant 3 to 4 times larger than that of SiO_2,[36,37] charge screening at the surface is much smaller for sapphire than for SiO_2, increasing the change in the measured WF. This combined effect of dipoles induced by charge transfer and oppositely directed static polarization is significant and should be considered in conjunction with dopant selection to exercise control over the electronic properties of TMDCs.

CONCLUSIONS

In conclusion, we have demonstrated a tunable, "bidirectional" WF modulation of MoS_2 by noncovalently doping the semiconductor with the organic dopants TTF and two BT derivatives. Spectroscopic and KPFM measurements provide compelling evidence for n-doping of MoS_2 by TTF and p-doping of MoS_2 by BT moieties. Notably, p-doping of MoS_2 with organic adsorbates while rarely reported, would be useful in the fabrication of p−n junctions on TMDCs. Using substrates with different dielectric properties significantly altered the magnitude of WF change after doping. For TTF doping, WF shifts increased from 0.27 to 1.24 eV when changing from SiO_2/Si to sapphire. We rationalize that this large difference in WF change arises from formation of induced dipoles and static polarization at the semiconductor/substrate interface. The ability to "bidirectionally" tune MoS_2 WF with different underlying substrates allows for production of electronically tailored TMDCs, which are needed for devices such as FETs and diodes. Moreover, such noncovalent doping by physisorption is scalable, reversible, and nondamaging to the semiconductor, making its use feasible for the development of next-generation TMDC devices.

DOI: 10.1021/acs.jpcc.8b10826
J. Phys. Chem. C XXXX, XXX, XXX−XXX

METHODS

Materials. Dimethylacetylene dicarboxylate was purchased from TCI chemicals. Methylamine (2.0 M in toluene), 1-hexylamine, carbon disulfide, and dimethylformamide (DMF), were purchased from Sigma-Aldrich and used as received. CVD MoS_2 samples were purchased from Six Carbon Technologies and 2D Layers.

Synthesis of ((*E*)-3,3′-Methyl-5,5′-bithiazolidinylidene-4,4′-dione). To a 20 mL scintillation vial, chilled to 0 °C in an ice bath, was added methylamine (2 equiv) in DMF. Carbon disulfide (2 equiv) was added dropwise and the resulting yellow/orange solution was stirred for 10 min. Dimethylacetylene dicarboxylate (1 equiv) was then added dropwise and the dark solution was stirred for an additional 10 min. The solution was then placed in a refrigerator and allowed to stand overnight. Red crystals precipitated from the solution and were collected by vacuum filtration and washed with methanol. The solid was dried under vacuum overnight to give the product in 30% yield (1.1 g). ^{1}H NMR (500 MHz, DMSO): δ 3.54 (s); ^{13}C NMR (126 MHz, $CDCl_3$): δ 194.71, 193.99, 187.45, 166.98, 160.41, 129.25, 125.02, 51.70, 32.08, 31.81, 31.25. **Peak doubling in the ^{13}C NMR was observed (potentially representing E/Z isomers). Mass spectroscopy confirms a single molecular ion peak. ESI-MS: calcd for $C_{12}H_{10}N_2O_2S_4$ [M^+], 290.3901; found, 312.9207 [M + Na].

Synthesis of ((*E*)-3,3′-Butyl-5,5′-bithiazolidinylidene-4,4′-dione). To a 20 mL scintillation vial, chilled to 0 °C in an ice bath was added *n*-butylamine (2 equiv) in DMF. Carbon disulfide (2 equiv) was added dropwise and the resulting yellow/orange solution was stirred for 10 min. Dimethylacetylene dicarboxylate (1 equiv) was then added dropwise and the dark solution was stirred for an additional 10 min. The solution was precipitated in cold methanol and the resulting orange crystals were collected by vacuum filtration and washed with methanol. The solid was dried under vacuum overnight to give the product in 45% yield (3.5 g). ^{1}H NMR (500 MHz, $CDCl_3$). δ (ppm): 4.13 (t, 4H, J = 7.6 Hz), 1.71 (t, 4H, J = 7.6 Hz), 1.40 (t, 4H, J = 7.5 Hz) 0.97 (t, 6H, J = 7.36 Hz). ^{13}C NMR (126 MHz, $CDCl_3$): δ 194.49 (C═S), 166.90 (C═O), 124.67 (C═C), 44.55, 29.12, 20.04, 13.65. MALDI-MS: calcd for $C_{14}H_{18}N_2O_2S_4$ [M^+], 374.0251; found, 374.792.

Doping. TTF and BT solutions were prepared at a concentration of 0.005 mg/mL in methanol. 100 μL of the solution was drop-cast onto MoS_2 using a pipette.

Cleaning up the Doped MoS_2. To clean the substrates, the doped MoS_2 was immersed into the 20 mL scintillation vials of chloroform followed by sonication for 5 min.

Kelvin Probe Force Microscopy. KPFM experiments were conducted on a Digital Instrument BioScope. The probes employed were AppNano ANSCM-PA Platinum-coated Si cantilever probes that have a resonance frequency of ~254 kHz. A mixed electrical excitation signal composed of a dc voltage and ac voltage was applied between the probe and the grounded sample. After a height scan of the substrate, the tip was lifted 40 nm above the sample to acquire the surface potential data. The scan rate was 0.4 Hz and the sampling density was 512 lines with 512 samples/line.

ASSOCIATED CONTENT

Supporting Information

The Supporting Information is available free of charge on the ACS Publications website at DOI: 10.1021/acs.jpcc.8b10826.

Height profile of a MoS_2 flake; surface height and SPC images with the SPC and height histograms, before and after merely drop-casting the solvent methanol on MoS_2; height and SPC images and corresponding histograms of a MoS_2 flake on both SiO_2/Si and sapphire as underlying substrates, after cleaning-up TTF, m-BT and b-BT; surface height and SPC images with histograms of monolayer MoS_2 before and after doping with butyl-BT, using two substrates of SiO_2/Si and sapphire; PL spectra and photodecay of m-BT in the background; PL spectra of TTF in the background; absorption spectrum of m-BT and TTF; matrix-assisted laser desorption/ionization time of flight mass spectrometry spectrum of butyl-BT; supplemental knowledge of the capacitive interaction between the tip and the sample (PDF)

AUTHOR INFORMATION

Corresponding Author

*E-mail: mdbarnes@chem.umass.edu.

ORCID

Todd Emrick: 0000-0003-0460-1797

Ashwin Ramasubramaniam: 0000-0001-6595-7442

Michael D. Barnes: 0000-0002-6201-7284

Author Contributions

$^{\perp}$P.W. and R.S. authors contributed equally to the manuscript.

Notes

The authors declare no competing financial interest.

ACKNOWLEDGMENTS

We thank Shaoyu Chen in Physics Dept. at UMass Amherst for the help in PL spectra measurements. Funding for this work was provided by the US Department of Energy and the National Science Foundation (NSF DMR-1808011).

REFERENCES

(1) Zhang, Z.-X.; Li, D. Novel p-n Junctions Based on Ambipolar Two-Dimensional Crystals. *Acta Phys. Sin.* **2017**, *66*, 217302 DOI: 10.7498/aps.66.217302.

(2) Fan, J.; Li, T.; Djerdj, I. Two-Dimensional Atomic Crystals: Paving New Ways for Nanoelectronics. *J. Electron. Mater.* **2015**, *44*, 4080−4097.

(3) Giannazzo, F.; Fisichella, G.; Greco, G.; Di Franco, S.; Deretzis, I.; La Magna, A.; Bongiorno, C.; Nicotra, G.; Spinella, C.; Scopelliti, M. Ambipolar MoS_2 Transistors by Nanoscale Tailoring of Schottky Barrier Using Oxygen Plasma Functionalization. *ACS Appl. Mater. Interfaces* **2017**, *9*, 23164−23174.

(4) Ryder, C. R.; Wood, J. D.; Wells, S. A.; Hersam, M. C. Chemically Tailoring Semiconducting Two-Dimensional Transition Metal Dichalcogenides and Black Phosphorus. *ACS Nano* **2016**, *10*, 3900−3917.

(5) Radisavljevic, B.; Radenovic, A.; Brivio, J.; Giacometti, V.; Kis, A. Single-Layer MoS_2 Transistors. *Nat. Nanotechnol.* **2011**, *6*, 147−150.

(6) Zhang, R.; Li, H.; Qu, Y.; Zhang, J.; Liu, J.; Han, Y. Authigenic Buffer Layer: Tuning Surface Work Function in All Polymer Blend Solar Cells. *Colloids Surf., A* **2017**, *535*, 149−156.

(7) Melitz, W.; Shen, J.; Kummel, A. C.; Lee, S. Kelvin Probe Force Microscopy and Its Application. *Surf. Sci. Rep.* **2011**, *66*, 1−27.

(8) Zhang, H.; Shang, M.-h.; Zheng, X.; Zeng, Z.; Chen, R.; Zhang, Y.; Zhang, J.; Zhu, Y. Ba^{2+} Doped $CH_3NH_3PbI_3$ to Tune the Energy State and Improve the Performance of Perovskite Solar Cells. *Electrochim. Acta* **2017**, *254*, 165−171.

(9) Mei, Y.; Fogel, D.; Chen, J.; Ward, J. W.; Payne, M. M.; Anthony, J. E.; Jurchescu, O. D. Interface Engineering to Enhance

DOI: 10.1021/acs.jpcc.8b10826
J. Phys. Chem. C XXXX, XXX, XXX−XXX

Charge Injection and Transport in Solution-Deposited Organic Transistors. *Org. Electron.* **2017**, *50*, 100−105.
(10) Lanzillo, N. A.; Simbeck, A. J.; Nayak, S. K. Strain Engineering the Work Function in Monolayer Metal Dichalcogenides. *J. Phys.: Condens. Matter* **2015**, *27*, 175501.
(11) Li, F.; Qi, J.; Xu, M.; Xiao, J.; Xu, Y.; Zhang, X.; Liu, S.; Zhang, Y. Layer Dependence and Light Tuning Surface Potential of 2D MoS_2 on Various Substrates. *Small* **2017**, *13*, 1603103.
(12) Zhang, Q.; Chen, Y.; Zhang, C.; Pan, C.-R.; Chou, M.-Y.; Zeng, C.; Shih, C.-K. Bandgap Renormalization and Work Function Tuning in $MoSe_2$/hBN/Ru(0001) Heterostructures. *Nat. Commun.* **2016**, *7*, 13843.
(13) Sandonas, L. M.; Gutierrez, R.; Pecchia, A.; Seifert, G.; Cuniberti, G. Tuning Quantum Electron and Phonon Transport in Two-Dimensional Materials by Strain Engineering: a Green's Function Based Study. *Phys. Chem. Chem. Phys.* **2017**, *19*, 1487−1495.
(14) Chen, W.; Santos, E. J. G.; Zhu, W.; Kaxiras, E.; Zhang, Z. Tuning the Electronic and Chemical Properties of Monolayer MoS_2 Adsorbed on Transition Metal Substrates. *Nano Lett.* **2013**, *13*, 509−514.
(15) Baik, S. S.; Im, S.; Choi, H. J. Work Function Tuning in Two-Dimensional MoS_2 Field-Effect-Transistors with Graphene and Titanium Source-Drain Contacts. *Sci. Rep.* **2017**, *7*, 45546.
(16) Sim, D. M.; Kim, M.; Yim, S.; Choi, M.-J.; Choi, J.; Yoo, S.; Jung, Y. S. Controlled Doping of Vacancy-Containing Few-Layer MoS_2 via Highly Stable Thiol-Based Molecular Chemisorption. *ACS Nano* **2015**, *9*, 12115−12123.
(17) Liu, X.; Qu, D.; Ryu, J.; Ahmed, F.; Yang, Z.; Lee, D.; Yoo, W. J. P-Type Polar Transition of Chemically Doped Multilayer MoS_2 Transistor. *Adv. Mater.* **2016**, *28*, 2345−2351.
(18) Ramasubramaniam, A.; Selhorst, R.; Alon, H.; Barnes, M. D.; Emrick, T.; Naveh, D. Combining 2D inorganic semiconductors and organic polymers at the frontier of the hard-soft materials interface. *J. Mater. Chem. C* **2017**, *5*, 11158−11164.
(19) Alon, H.; Stern, C.; Kirshner, M.; Sinai, O.; Wasserman, M.; Selhorst, R.; Gasper, R.; Ramasubramaniam, A.; Emrick, T.; Naveh, D. Lithographically Patterned Functional Polymer-Graphene Hybrids for Nanoscale Electronics. *ACS Nano* **2018**, *12*, 1928−1933.
(20) Selhorst, R. C.; Puodziukynaite, E.; Dewey, J. A.; Wang, P.; Barnes, M. D.; Ramasubramaniam, A.; Emrick, T. Tetrathiafulvalene-Containing Polymers for Simultaneous Non-Covalent Modification and Electronic Modulation of MoS_2 Nanomaterials. *Chem. Sci.* **2016**, *7*, 4698−4705.
(21) Wang, H.; Yu, L.; Lee, Y.-H.; Shi, Y.; Hsu, A.; Chin, M. L.; Li, L.-J.; Dubey, M.; Kong, J.; Palacios, T. Integrated Circuits Based on Bilayer MoS_2 Transistors. *Nano Lett.* **2012**, *12*, 4674−4680.
(22) Jariwala, D.; Sangwan, V. K.; Lauhon, L. J.; Marks, T. J.; Hersam, M. C. Emerging Device Applications for Semiconducting Two-Dimensional Transition Metal Dichalcogenides. *ACS Nano* **2014**, *8*, 1102−1120.
(23) Mouri, S.; Miyauchi, Y.; Matsuda, K. Tunable Photoluminescence of Monolayer MoS_2 via Chemical Doping. *Nano Lett.* **2013**, *13*, 5944−5948.
(24) Nasiri, F.; Zolali, A.; Asadbegi, S. Solvent-free One-pot Synthesis of 2,2′-dithioxo-[5,5′]bithiazolidinylidene-4,4′-diones. *J. Heterocycl. Chem.* **2015**, *53*, 989−992.
(25) Palermo, V.; Palma, M.; Samorì, P. Electronic Characterization of Organic Thin Films by Kelvin Probe Force Microscopy. *Adv. Mater.* **2006**, *18*, 145−164.
(26) Baghgar, M.; Barnes, A. M.; Pentzer, E.; Wise, A. J.; Hammer, B. A. G. Morphology-Dependent Electronic Properties in Cross-Linked (P3HT-b-P3MT) Block Copolymer Nanostructures. *ACS Nano* **2014**, *8*, 8344−8349.
(27) Baghgar, M.; Barnes, M. D. Work Function Modification in P3HT H/J Aggregate Nanostructures Revealed by Kelvin Probe Force Microscopy and Photoluminescence Imaging. *ACS Nano* **2015**, *9*, 7105−7112.
(28) Wang, P.; Barnes, M. D. Disentangling "Bright" and "Dark" Interactions in Ordered Assemblies of Organic Semiconductors. *Nano Lett.* **2017**, *17*, 6949−6953.
(29) Liscio, A.; Palermo, V.; Fenwick, O.; Braun, S.; Müllen, K.; Fahlman, M.; Cacialli, F.; Samorí, P. Local Surface Potential of π-Conjugated Nanostructures by Kelvin Probe Force Microscopy: Effect of the Sampling Depth. *Small* **2011**, *7*, 634−639.
(30) Liscio, A.; Bonini, M.; Treossi, E.; Orgiu, E.; Kastler, M.; Dötz, F.; Palermo, V.; Samorì, P. Improving Charge Transport in Poly(3-hexylthiophene) Transistors via Blending with an Alkyl-Substituted Phenylene-Thiophene-Thiophene-Phenylene Molecule. *J. Polym. Sci., Part B: Polym. Phys.* **2012**, *50*, 642−649.
(31) Liscio, A.; Palermo, V.; Samorì, P. Nanoscale Quantitative Measurement of the Potential of Charged Nanostructures by Electrostatic and Kelvin Probe Force Microscopy: Unraveling Electronic Processes in Complex Materials. *Acc. Chem. Res.* **2010**, *43*, 541−550.
(32) Li, Y.; Qi, Z.; Liu, M.; Wang, Y.; Cheng, X.; Zhang, G.; Sheng, L. Photoluminescence of monolayer MoS_2 on $LaAlO_3$ and $SrTiO_3$ substrates. *Nanoscale* **2014**, *6*, 15248−15254.
(33) Mak, K. F.; He, K.; Lee, C.; Lee, G. H.; Hone, J.; Heinz, T. F.; Shan, J. Tightly Bound Trions in Monolayer MoS_2. *Nat. Mater.* **2012**, *12*, 207−211.
(34) Naveh, D. to be published.
(35) Jeong, K. S.; Deng, Z.; Keuleyan, S.; Liu, H.; Guyot-Sionnest, P. Air-Stable n-Doped Colloidal HgS Quantum Dots. *J. Phys. Chem. Lett.* **2014**, *5*, 1139−1143.
(36) Krupka, J.; Derzakowski, K.; Tobar, M.; Hartnett, J.; Geyer, R. G. Complex Permittivity of Some Ultralow Loss Dielectric Crystals at Cryogenic Temperatures. *Meas. Sci. Technol.* **1999**, *10*, 387−392.
(37) Rong, L.-m.; Meng, Z.-j.; Xiao, C.; Zhou, L.; Du, L.-h.; Liu, K.; Du, J.-f. Impact of Defects on Local Optical Dielectric Properties of Si/SiO_2 Interfaces by Layered Capacitor Modeling. *Appl. Phys. A: Mater. Sci. Process.* **2016**, *122*, 283.

DOI: 10.1021/acs.jpcc.8b10826
J. Phys. Chem. C XXXX, XXX, XXX−XXX